

Theoretical Calculation of Bond Dissociation Energies and Enthalpies of Formation for Halogenated Molecules

Yannis G. Lazarou*

Institute of Physical Chemistry, National Center for Scientific Research "Demokritos", Aghia Paraskevi 153 10, Attiki, Greece

Alexandros V. Prosmittis, Vassileios C. Papadimitriou, and Panos Papagiannakopoulos

Department of Chemistry, University of Crete, Heraklion 714 09, Crete, Greece

Received: January 25, 2001; In Final Form: April 16, 2001

The bond dissociation energies and the enthalpies of formation of halogenated molecules were theoretically calculated, and the results were compared with the corresponding experimental values in order to examine the reliability of a large number of levels of theory in thermochemical calculations. Density functional theory using a multitude of exchange and correlation functionals, Møller–Plesset perturbation theory, and QCISD(T) and CCSD(T) methods were employed, with all-electron and effective-core potential basis sets of varying complexity. A small set of 19 molecules was selected, consisting of X_2 , HX, and CH_3X ($X = F, Cl, Br,$ and I), the mixed-halogen molecules ClF, BrF, BrCl, IF, and ICl, and H_2 and CH_4 . The calculated bond dissociation energies were corrected for basis set superposition errors and the first-order spin–orbit coupling in the 2P state of halogen atoms. In addition, the enthalpies of formation of all molecules in the set as well as those of methyl CH_3 and halomethyl radicals CH_2X were also calculated by using the corresponding atomization reactions, corrected for the spin–orbit coupling in the 3P state of carbon atom and the 2P state of halogen atoms. Levels of theory employing the B3P86 functional with moderately large basis sets, augmented with diffusion and polarization functions, were found to be sufficiently reliable in the calculation of bond dissociation energies of closed-shell halogenated molecules. In particular, the B3P86/6-311++G(2df,p) level of theory was found to be the most accurate, with an RMS deviation of 6 kJ mol^{-1} for 23 bond dissociation energies, with a negligible dependence of the accuracy on the level of theory chosen for the geometry optimization. In addition, the B3P86 functional in combination with small basis sets was found to be superior to B3LYP and MP2 in the calculation of molecular structures. Regarding the calculated enthalpies of formation, G2 theory was the most accurate, with an RMS deviation of 9 kJ mol^{-1} , followed by several combinations of the B3PW91 and B3LYP functionals with mostly large basis sets. However, the B3P86 functional tends to overbind open-shell species, resulting in an underestimation of the enthalpies of formation for polyatomic molecules. Extension of the bond dissociation energy calculations at levels of theory employing the B3P86 functional to a larger set of 60 bonds in 41 halogen-containing molecules revealed systematic errors dependent on the molecular size. Therefore, the calculated bond dissociation energies at the B3P86/6-311++G(2df,p) level of theory were empirically improved by increasing the absolute energies of the radicals by the quantity $9 \times 10^{-5} \cdot N_e$ Hartrees (N_e = total number of electrons of the radical), with a subsequent lowering of the RMS deviation in the larger set to 8.0 kJ mol^{-1} .

Introduction

In the past decade, halogenated species have been extensively investigated, due to their potential significance in processes affecting our environment, such as stratospheric ozone depletion and global warming. Halogen-containing molecules are constantly released into the atmosphere by natural as well as anthropogenic emissions, leading to serious environmental quality concerns. The fate of halogen-containing molecules in the troposphere is primarily governed by their reactions with OH radicals and, to a lesser extent, with NO_3 radicals at nighttime as well as with Cl atoms in the marine environment.^{1–3} Sunlight photolysis, for those molecules containing halogen atoms heavier than fluorine, constitutes the initial step of their degradation at stratospheric levels, accompanied by the production of halogen atoms which catalytically destroy stratospheric

ozone.^{4,5} Due to the relatively weak C–Br and C–I bonds, sunlight photolysis at longer wavelengths is an additional pathway of the tropospheric degradation of bromine-containing molecules and the primary decomposition pathway for iodine-containing molecules. Therefore, the modeling of their atmospheric chemistry requires the photolysis cross sections as a function of the absorbed photon wavelength and the rate constants with atmospheric oxidants at a relatively wide range of temperatures.⁶ In most cases, hydrogen-containing halogenated molecules react with atmospheric oxidants (OH, NO_3 , Cl) via the metathesis of a hydrogen atom. It has been shown that the rate constants for hydrogen atom abstraction in halogenated alkanes are correlated to their C–H bond strengths,^{7–9} leading to simple rules allowing the crude assessment of their atmospheric reactivity. In addition, the strength of the C–X bonds in halogenated alkanes is directly related to their photolytic

instability and the energetically accessible pathways for the initial photolysis step.

Only a small number of bond dissociation energies of halogenated molecules have been experimentally determined, and the scarcity of experimental data is particularly severe for bromine and iodine containing molecules.^{6,10,11} However, present-day electronic computers technology, combined with progress made in electronic structure theory, have increased the number of theoretical studies aiming to derive thermochemical properties for chemical compounds otherwise difficult or impossible to measure. In a number of recent theoretical studies, the thermochemical properties of several important halogenated molecules have been calculated employing various high-quality levels of theory.^{12–20} Fluorinated molecules have attracted the greatest attention, since they have been proposed as alternative ozone-friendly refrigerant and fire-suppressing agents, while at the other end, theoretical studies on iodinated species are rare. However, it must be noted that theoretical calculations on systems containing iodine are impeded by the large size of the iodine atom, prohibiting the use of sophisticated computer-intensive electron-correlation methods and extended basis sets.

In the present study, the examination of a large number of levels of theory in the determination of experimentally known bond dissociation energies and enthalpies of formation ($\Delta_f H^\circ$) at 298.15 K for small halogenated molecules was undertaken, giving particular emphasis on the computational efficiency. A small set of molecules was selected for the benchmark calculations, consisting of the halogen molecules X_2 ($X = F, Cl, Br,$ and I), mixed-halogen molecules ($ClF, BrF, BrCl, IF,$ and ICl), hydrogen halides HX , and halomethanes CH_3X ($X = F, Cl, Br,$ and I), whose bond dissociation energies were computed from the enthalpies of formation experimentally available for molecules and the corresponding radicals.^{6,10,11,21,22} In addition, H_2 and CH_4 were included in the set, since their enthalpies of formation and their $H-H$ and $C-H$ bond dissociation energies are accurately known.^{6,10,11} To further assess the performance of the levels of theory employed in this study, we also derived the enthalpies of formation of the above molecules as well as those of methyl CH_3 and halomethyl radicals CH_2X . The bond dissociation energies were corrected for basis set superposition errors (BSSE) and the first-order spin-orbit splitting of the 2P state of halogen atoms. Similarly, the enthalpies of formation were corrected for the first-order spin-orbit splitting of the 3P state of carbon atom and the 2P state of halogen atoms.

Electron-correlation was treated by density functional theory,^{23–27} employing a large number of exchange and correlation functionals and the Møller–Plesset perturbation theory (MP2, MP4),^{28–30} and by quadratic CI³¹ and coupled-cluster methods,^{32,33} including single, double, and perturbative triple excitations (QCISD(T), CCSD(T)). Several variants of all-electron (AE) basis sets were employed, ranging from the fairly small 3-21G^{34,35} and SVP³⁶ basis sets to the larger 6-311G^{37,38} and correlation-consistent basis sets.^{39–42} In addition, the Los-Alamos double- ζ (LanL2DZ),^{43,44} Stuttgart group (SDD and SDDAll),⁴⁵ and compact (CEP-31 and CEP-121)⁴⁶ effective core potentials (ECP) were also employed, augmented with diffusion and polarization functions. The use of effective core potentials is particularly significant in calculations involving the heavy bromine and iodine atoms, since the relativistic effects of the fast-moving inner electrons have already been taken into account, and being more compact, these basis sets tend to be more computationally effective than their all-electron counterparts.

Finally, the calculation of the bond dissociation energies for a number of larger halogenated molecules was performed by using the most reliable levels of theory obtained from the benchmark calculations. The results were compared with the experimental data available, and deviations appearing to be systematic were empirically corrected.

Computational Procedure

All theoretical calculations in the present work were carried out by the Gaussian94⁴⁷ and Gaussian98⁴⁸ program suites. Restricted Hartree–Fock (RHF–SCF) wave functions were used for all closed-shell species, and unrestricted Hartree–Fock (UHF–SCF) wave functions were used for the free radical species. The frozen-core approximation was used in all post-SCF electron correlation methods (MP2 and MP4SDQ, quadratic CI and coupled-cluster). In most cases, pure d- and f- functions were used, with the exception of the variants of the 3-21G and 6-31G basis sets (using 6 Cartesian d- functions) and the valence part of the SDD, CEP-31, and CEP-121 effective core potential (using 6 and 10 Cartesian d- and f- functions, respectively). The triple- ζ quality 6-311G basis set for iodine¹⁶ and the correlation-consistent basis sets for bromine⁴² were obtained from the Extensible Computational Chemistry Environment Basis Set Database.⁴⁹ The correlation-consistent basis sets for iodine^{50,51} were kindly provided by L. Visscher.⁵²

The exponents of diffusion and polarization functions used with the 6-311G basis set as well as those for bromine and iodine associated with the Los Alamos (LanL2DZ) and Stuttgart group (SDD) ECPs were those specified in the literature.¹⁶ The diffusion and polarization function exponents for the lighter elements (H, C, F, and Cl) used with the ECPs were separately determined. Thus, single-point energy calculations employing MP2, B3LYP, and B3P86 electron-correlation methods were performed by using the experimental geometries¹¹ of H_2 , OH, and HF for hydrogen, CH and C_2 for carbon, HF and F_2 for fluorine, and HCl and Cl_2 for chlorine at various levels of theory, and the optimal exponents were determined by total electronic energy minimization criteria. For hydrogen, the calculations were performed by using the LanL2DZG(d,p) and LanL2DZG-(d,pd) basis sets to determine the exponents of the p and d polarization functions, respectively. The optimal p and d exponents derived for hydrogen were different for each specific molecule and correlation method employed, with average values of 0.70 ± 0.5 and 0.8 ± 0.6 , respectively, being quite close to the exponents associated with the triple- ζ quality 6-311G basis set, 0.75 and 1.0, respectively. For the heavier elements, the optimal d and f polarization function exponents were calculated by using the LanL2DZG(d,p) and LanL2DZG(df,p) basis sets. The d polarization function exponents determined for C, F, Cl, Br, and I (those associated with the 6-311G basis set are noted in parentheses) were found to be 0.675 ± 0.15 (0.626), 1.226 ± 0.40 (1.750), 0.657 ± 0.17 (0.750), 0.395 ± 0.04 (0.451), and 0.264 ± 0.03 (0.302), respectively. Similarly, the optimal f polarization function exponents for C, F, Cl, Br, and I were found to be 0.829 ± 0.05 (0.800), 1.493 ± 0.41 (1.850), 0.709 ± 0.11 (0.700), 0.504 ± 0.06 (0.560), and 0.412 ± 0.05 (0.380), respectively. Multiple d (2d, 3d) and f (2f) polarization functions were constructed by multiplying the singly optimized exponent α of each function by a geometric progression of a number n (αn and α/n), and the value of n was appropriately optimized for each element and each type of function. Therefore, for hydrogen, the pair of two p functions (2p) was created by using an optimal value of $n_{2p} = 2$. For the second- and third-row elements C, F, and Cl, the optimal values of n_{2d} , n_{3d} , and n_{2f}

were calculated to be 2, 3, and 1.5, respectively for the (2d), (3d) and (2f) splittings. For Br and I, the corresponding optimal values were calculated to be 1.5, 2, and 1.5, respectively.

The exponents of the diffusion functions (an S shell for hydrogen and an SP shell for the elements C, F, and Cl) were appropriately optimized by using the anions H^- and OH^- (in its experimental geometry) for H and the atomic anions C^- , F^- , and Cl^- , respectively. The LanL2DZ++G(d,p) basis set was employed, using the MP2, B3LYP, and B3P86 electron-correlation methods. The optimized exponents (those associated with the 6-311G basis set are shown in parentheses) were found to be 0.0467 ± 0.016 (0.0360), 0.0307 ± 0.008 (0.0438), 0.0289 ± 0.0004 (0.1076), and 0.0500 ± 0.003 (0.0483) for H, C, F, and Cl, respectively. However, the diffusion functions for Br and I were comprised by a set of separate S and P functions with exponents reported previously.¹⁶

Generally, the optimal exponents calculated for the polarization and diffusion functions of the valence part of the LanL2DZ ECP are close to those available for the 6-311G basis set. Furthermore, their dependence on the molecular system and the correlation method employed in the optimization process is rather large (especially for fluorine); thus, the choice of their optimal values is obviously not straightforward. Therefore, for simplicity, the exponents associated for the polarization and diffusion functions of the 6-311G basis set were also employed for augmenting the valence part of the ECP's. In addition, the dependence of the bond dissociation energies on the exponents themselves was derived by performing calculations employing several DFT methods and the LanL2DZ++G(3d2f,2pd) basis set by using the exponents optimized by the above procedure. As will be shown later, the corresponding differences were small (ca. 0.2 kJ mol^{-1} in the computed bond dissociation energies at the B3P86/LanL2DZ++G(3d2f,2pd) level of theory), which suggests that the polarization and diffusion functions exponents of the 6-311G basis set constitute an equally acceptable choice to augmenting the valence part of the ECP basis sets.

The geometry optimization and the calculation of the vibrational frequencies for all species was performed at the MP2/6-311G(d) level of theory. Subsequently, all species were reoptimized and their frequencies evaluated at several levels of theory to assess the dependence of the optimization level on the accuracy of the bond dissociation energies derived. The vibrational frequencies were always scaled by a factor dependent on the level of theory employed for their calculation, obtained by a least-squares fit of the calculated versus the experimental vibrational frequencies for all closed-shell species and the CH_3 radical.¹¹ The factor used to scale down the MP2/6-311G(d) frequencies was found to be 0.9872. The zero-point energies and the corresponding thermal corrections to the enthalpy at 298.15 K were obtained by using the harmonic oscillator and rigid rotor approximations and were subsequently added to the absolute electronic energies, derived by the single-point energy calculations, to determine the corresponding total enthalpies and, consequently, the bond dissociation energies and the enthalpies of formation.

The bond dissociation energies calculated at each level of theory were corrected for basis set superposition errors (BSSE) by performing the corresponding counterpoise calculations.⁵³ Additional corrections to the calculated bond dissociation energies had to be applied for the first-order spin-orbit coupling effects of the doublet ground state (^2P) of halogen atoms. These corrections were taken to be the energy difference between the spin-orbit coupled ground state and the weighted J-averaged state, while the energy differences between J states were taken

from standard tables of atomic energy levels.⁵⁴ Thus, the total energy for the halogen atoms was lowered by 1.6, 3.5, 14.7, and 30.3 kJ mol^{-1} for F, Cl, Br, and I, respectively.

The calculations using the G2 compound method^{55,56} were performed using the MP2/6-311G(d) geometries and vibrational frequencies by computing the absolute electronic energy directly at the QCISD(T)/6-311+G(3df,2p) level of theory and subtracting the empirical corrections 0.00019 and 0.00481 hartrees for every valence α and β electron, respectively.

The accuracy of each level of theory was assessed by using the root-mean-square (RMS) deviation of the differences between the calculated and the experimentally available values for the entire set of bond dissociation energies or enthalpies of formation. In addition, the mean absolute deviation (MAD), the average deviation (AVD) and the maximum negative and positive deviations (MND and MPD, respectively) were also computed. MAD has been traditionally employed in the assessment of the reliability of theoretical methods,^{17,19,57} while the latter three criteria indicate the degree of balancing of errors for all members of the set, revealing systematic trends toward over- or underestimation of the property calculated.

Results and Discussion

The structural parameters and the vibrational frequencies (unscaled) for all species, calculated at the MP2/6-311G(d) level of theory, as well as the corresponding experimentally determined quantities^{11,58,59} are presented in Table 1. The average deviations for the bond lengths and the bond angles were 1.5% and 1.0%, respectively. It must be noted that for halomethyl radicals, two different stationary points could be obtained, one of which is planar. However, the planar structure for CH_2F and CH_2Cl possessed an imaginary frequency corresponding to the saddle point for umbrella inversion on the MP2/6-311G(d) potential energy surface. The difference between the MP2/6-311G(d) energies for the two stationary points was less than 0.1 kJ mol^{-1} for all radicals except CH_2F , whose bent structure is more stable by 3.2 kJ mol^{-1} . Furthermore, the difference of their corresponding single-point energies at the B3P86/6-311++G(2df,p), B3P86/6-311++G(3df,2p), and CCSD(T)/cc-pVDZ levels of theory were also small, on the order of 0.2 kJ mol^{-1} , with the exception of CH_2F at the CCSD(T)/cc-pVDZ level, whose bent structure is more stable by 2.4 kJ mol^{-1} . Similar small energetic differences between the planar and the bent structure were noticed for the CH_2Br radical at much higher levels of theory employing B3LYP, MP2, and CCSD(T) methods with TZ2P and 6-311++G(3df,3pd) basis sets.⁵⁹

Since the task of calculating the bond dissociation energies for all possible combinations of electron correlation methods with basis sets of various sizes would require enormous computational abilities, the calculations were initially performed using a small number of all-electron and ECP basis sets in combination with CCSD(T), QCISD(T), and most DFT electron correlation methods available. These preliminary results indicated the superiority of the P86 correlation functional, and therefore, many additional levels of theory were examined using a greater range of basis sets combined with a rather limited number of DFT methods containing the P86 as well as the LYP and PW91 correlation functionals, since the latter are employed by the most common B3LYP and B3PW91 methods. Thus, the bond dissociation energies at 298.15 K, corrected for BSSE and the spin-orbit coupling for halogen atoms, were calculated at more than 800 different levels of theory. The results for levels of theory possessing RMS errors below 14 kJ mol^{-1} are presented in Table 2, while selected results for less accurate

TABLE 1: Structural Parameters and Vibrational Frequencies (Unscaled), Calculated at the MP2/6-311G(d) Level of Theory for All Benchmark Species of the Present Study (Bond Lengths in Å, Angles in deg)

molecule	structural parameters		vibrational Frequencies	
	calculated	experimental ^a	calculated	experimental ^b
H ₂	H-H = 0.737	H-H = 0.741	4458	4401
F ₂	F-F = 1.412	F-F = 1.412	917	917
Cl ₂	Cl-Cl = 2.028	Cl-Cl = 1.988	538	560
Br ₂	Br-Br = 2.302	Br-Br = 2.281	330	325
I ₂	I-I = 2.714	I-I = 2.666	222	215
HF	H-F = 0.918	H-F = 0.917	4092	4138
HCl	H-Cl = 1.284	H-Cl = 1.275	2951	2990
HBr	H-Br = 1.429	H-Br = 1.414	2630	2649
HI	H-I = 1.639	H-I = 1.609	2289	2309
CH ₃	C-H = 1.078 ∠H-C-H = 120.00 ∠H-C(-H)-H = 180.00	C-H = 1.079 ∠H-C-H = 120.00 ∠H-C(-H)-H = 180.00	430, 1453(2), 3173, 3366(2)	606, 1402(2), 3004, 3161(2)
CH ₄	C-H = 1.088 ∠H-C-H = 109.47 ∠H-C(-H)-H = 120.00	C-H = 1.087 ∠H-C-H = 109.47 ∠H-C(-H)-H = 120.00	1385(3), 1605(2), 3082, 3219(3)	1306(3), 1534(2), 2917, 3019(3)
CH ₂ F	C-F = 1.342 C-H = 1.081 ∠H-C-F = 114.06 ∠H-C(-F)-H = 148.10	-	731, 1199, 1214, 1524, 3192, 3351	260, 1170
CH ₃ F	C-F = 1.384 C-H = 1.090 ∠H-C-F = 108.93 ∠H-C(-F)-H = 120.00	C-F = 1.382 C-H = 1.095 ∠H-C-F = 108.5 ∠H-C(-F)-H = 120.00	1098, 1228(2), 1545(3), 3093, 3195(2)	1049, 1182(2), 1464, 1467(2), 2930, 3006(2)
CH ₂ Cl	C-Cl = 1.703 C-H = 1.077 ∠H-C-Cl = 117.25 ∠H-C(-Cl)-H = 164.38	-	309, 872, 1051, 1474, 3230, 3386	402, 827, 1391
CH ₃ Cl	C-Cl = 1.780 C-H = 1.087 ∠H-C-Cl = 108.81 ∠H-C(-Cl)-H = 120.00	C-Cl = 1.785 C-H = 1.090 ∠H-C-Cl = 108.1 ∠H-C(-Cl)-H = 120.00	776, 1077(2), 1454, 1522(2), 3121, 3232(2)	732, 1017(2), 1355, 1452(2), 2937, 3039(2)
CH ₂ Br	C-Br = 1.855 C-H = 1.078 ∠H-C-Br = 117.39 ∠H-C(-Br)-H = 163.16	C-Br = 1.845 C-H = 1.086 ∠H-C-Br = 118.00 ∠H-C(-Br)-H = 180.00	323, 728, 977, 1445, 3223, 3379	368, 693, 953, 1356
CH ₃ Br	C-Br = 1.940 C-H = 1.086 ∠H-C-Br = 108.28 ∠H-C(-Br)-H = 120.00	C-Br = 1.933 C-H = 1.086 ∠H-C-Br = 107.7 ∠H-C(-Br)-H = 120.00	642, 1003(2), 1397, 1517(2), 3129, 3246(2)	611, 955(2), 1306, 1443(2), 2935, 3056(2)
CH ₂ I	C-I = 2.055 C-H = 1.079 ∠H-C-I = 118.40 ∠H-C(-I)-H = 169.91	-	173, 639, 902, 1423, 3221, 3375	375, 611, 1331, 3050
CH ₃ I	C-I = 2.153 C-H = 1.086 ∠H-C-I = 108.17 ∠H-C(-I)-H = 120.00	C-I = 2.132 C-H = 1.084 ∠H-C-I = 107.7 ∠H-C(-I)-H = 120.00	551 936(2), 1351, 1510(2), 3125, 3245(2)	533, 882(2), 1252, 1436(2), 2933, 3050(2)
ClF	Cl-F = 1.673	Cl-F = 1.628	734	786
BrF	Br-F = 1.802	Br-F = 1.759	644	671
BrCl	Br-Cl = 2.168	Br-Cl = 2.136	440	444
IF	I-F = 1.969	I-F = 1.910	595	610
ICl	I-Cl = 2.369	I-Cl = 2.321	379	384

^a Experimental structural data for diatomic molecules taken from ref 11 for alkyl halides, ref 58 for CH₄ and CH₃, and ref 59 for CH₂Br.
^b Experimental vibrational frequencies taken from ref 11 (those for halomethyl radicals are not completely known).

but particularly interesting levels of theory are presented in Table 3. The experimental bond dissociation energies were computed from the corresponding enthalpies of formation experimentally available. Most values were obtained from the NIST-JANAF Thermochemical tables,^{10,11} except those for halomethyl radicals,⁶ CH₃Br,²¹ and CH₃I.²²

As can be seen in Table 2, the hybrid B3P86 functional^{60,61} is reproducing the bond dissociation energies of the benchmark molecules in this study with an outstanding accuracy for a wide range of basis sets, greatly surpassing the most commonly used B3LYP^{62,63,64} and B3PW91^{65,66} functionals. The dependence of the accuracy on the details of the basis set is harder to assess, particularly since the sample of 23 bond dissociation energies

in a set of 19 molecules is rather small and furthermore, the differences among the levels of theory employing B3P86 and various basis sets are smaller than the typical uncertainty of ca. 8 kJ mol⁻¹ for the experimental values. However, the accuracy of the B3P86 calculations increases with the size of the basis set, tending to improve in the presence of polarization functions, as has been frequently noted.^{57,67,68} The performance of the triple- ζ correlation-consistent cc-pVTZ basis sets rivals that of the Pople-style augmented 6-311G basis sets, and furthermore, the use of the highly extended and costly correlation-consistent AUG-cc-pVTZ basis set for iodine does not offer any improvement over its 6-311+G(3df) counterpart. The accuracy of effective core potentials (augmented with polarization and

TABLE 2: Root Mean Square Deviation (RMS), Mean Absolute Deviation (MAD), Average Deviation (AVD), Maximum Negative and Positive Deviations (MND, MPD), and Basis Set Superposition Error (BSSE) at Levels of Theory Possessing RMS Deviation Less than 14 kJ mol⁻¹ for the Bond Dissociation Energies at 298.15 K of All Benchmark Species

level of theory	RMS	MAD	AVD	MND	MPD	BSSE
B3P86/6-311++G(2df,p)	5.8	4.0	-1.2	-20.1	8.6	-2.1
B3P86/6-311++G(3df,2p)	6.1	4.8	0.5	-17.6	9.7	-2.1
B3P86/3-21++G(3df,2p)	6.3	4.6	-1.8	-16.6	9.0	-11.0
B3P86/SCFT-6-311++G(2df,p) ^a	6.3	4.3	-1.7	-21.5	8.6	-2.2
B3P86/SCFT-6-311++G(3df,2p)	6.5	5.0	-0.1	-19.1	9.7	-2.4
B3P86/3-21++G(2df,p)	6.7	5.2	-2.9	-13.2	8.1	-18.7
B3P86/LanL2DZ++G(3df,2pd)	6.8	5.7	-1.7	-14.5	10.2	-0.9
B3P86/AUG-cc-pVTZ_I/6-311+G(3df) ^b	7.0	5.2	-0.3	-23.4	9.7	-1.4
B3P86/AUG-cc-pVTZ_I/6-311+G(2df)	7.1	5.3	-0.3	-23.4	9.7	-1.4
B3P86/cc-pVTZ	7.1	4.9	-0.8	-24.6	9.9	-1.0
B3P86/AUG-cc-pVQZ_I/6-311+G(3df)	7.1	5.6	0.7	-21.9	10.3	-1.5
B3P86/SCFT-LanL2DZ++G(3d2f,2pd)	7.3	6.1	-1.8	-16.0	10.2	-1.4
B3P86/LanL2DZ++G(3d2f,p)	7.3	5.8	-2.6	-17.1	9.0	-1.1
B3P86/AUG-cc-pV5Z_I/6-311+G(3df)	7.4	6.0	1.4	-21.1	11.4	-1.6
B3P86/LanL2DZ++G(3d2f,2p)	7.4	6.1	-1.9	-17.1	10.2	-1.2
B3P86/AUG-cc-pVTZ	7.5	5.4	-0.4	-29.6	9.7	-1.1
B3P86/6-311++G(3df,3pd)	7.5	5.5	-0.5	-25.1	9.8	-2.6
B3P86/LanL2DZ++G(3d2f,2pd)	7.6	6.2	-2.2	-17.1	10.2	-1.4
B3P86/SDD++G(3d2f,2pd)	7.7	5.6	-0.5	-24.9	10.5	0.1
B3P86/LanL2DZ-OPT(++G(3d2f,2pd)) ^c	7.7	6.0	-2.7	-18.9	9.5	-1.8
B3P86/LanL2DZ+G(3d2f,2p)	8.3	6.6	-1.4	-17.1	19.4	-3.4
B3P86/LanL2DZ++G(2df,p)	8.5	6.3	-4.3	-21.3	9.0	-1.3
B3P86/LanL2DZ+G(3df,2p)	8.9	7.0	-2.2	-18.8	19.4	-3.7
B3P86/SDD++G(2df,p)	8.9	5.5	-3.3	-30.4	9.0	0.1
B3P86/AUG-cc-pVTZ_I/6-311+G(d)	9.4	6.4	-1.3	-29.6	9.7	-1.1
B3P86/6-311++G(2d,p)	10.0	7.5	-5.1	-30.5	8.6	-2.0
B3P86/CEP-121++G(2df,p)	11.4	9.8	-8.2	-19.7	8.6	-0.3
B3P86/SDDAll++G(3d2f,2pd)	11.6	8.9	-7.4	-36.0	10.5	-0.1
B3P86/CEP-31++G(2df,p)	12.1	10.5	-8.8	-19.7	9.0	-0.8
BHandH/LanL2DZ+G(3d2f,2p)	12.2	8.9	1.6	-28.4	25.1	-3.7
B3P86/AUG-cc-pVDZ_I/6-311+G(d)	12.4	9.3	-8.5	-32.6	5.2	-2.1
BHandH/LanL2DZ++G(3d2f,2pd)	12.5	9.3	1.0	-28.4	25.1	-1.3
BHandH/LanL2DZ++G(3d2f,2p)	12.5	9.3	1.0	-28.4	25.3	-1.2
BHandH/LanL2DZ++G(3d2f,p)	12.5	9.2	0.6	-28.4	25.6	-1.1
BHandH/LanL2DZ+G(3df,2p)	12.6	9.3	0.7	-30.3	24.7	-3.8
BHandH/LanL2DZ++G(3df,2pd)	12.8	9.6	0.5	-30.3	24.9	-1.3
BHandH/3-21++G(2df,p)	13.1	10.1	3.3	-28.9	29.0	-18.2
BHandH/LanL2DZ++G(2df,p)	13.2	10.1	-1.3	-30.5	23.9	-1.2
B3PW91/AUG-cc-pV5Z_I/6-311+G(3df)	13.3	11.6	-11.6	-33.7	-2.3	-1.6
BHandH/SDDAll++G(3d2f,2pd)	13.6	9.8	-1.5	-36.6	25.4	-0.6
B3PW91/6-311++G(3df,2p)	13.6	12.5	-12.5	-30.5	-6.2	-2.0
B3P86/AUG-cc-pVDZ_I/6-311+G(d)	13.7	9.3	0.8	-19.1	46.1	-2.3
BHandH/3-21++G(3df,2p)	13.7	11.0	4.2	-29.1	25.9	-11.0
B3PW91/AUG-cc-pVQZ_I/6-311+G(3df)	13.8	12.3	-12.3	-34.6	-4.8	-1.5
B3P86/SDDAll++G(2df,p)	13.9	10.8	-9.9	-41.2	9.0	-0.4
BHandH/CEP-31++G(2df,p)	13.9	10.4	-3.1	-34.4	15.6	-0.7
BHandH/CEP-121++G(2df,p)	14.0	10.6	-2.8	-34.3	16.2	-0.4

^a Symbol SCFT used to denote tight SCF wave function convergence criteria (RMS density matrix to 10⁻⁸, MAX density matrix to 10⁻⁶).

^b Symbol _I/basisset used to denote a specific basis set for iodine (different from the one used for the other atoms). ^c Symbol -OPT(basis set) is used to denote that the exponents of diffusion and polarization functions associated with the LanL2DZ basis set were obtained from an exponent optimization procedure.

diffusion functions) parallels that of all-electron basis sets, as can be seen in Tables 2 and 3 for the B3P86, B3PW91, and B3LYP functionals. Moreover, the use of separately optimized exponents for the polarization and diffusion functions with the LanL2DZ ECP (denoted by the symbol -OPT) has a minor effect on the overall accuracy, and the difference between the RMS deviations for the B3P86/LanL2DZ++G(3d2f,2pd) and B3P86/LanL2DZ-OPT(++G(3d2f,2pd)) levels of theory is ca. 0.2 kJ mol⁻¹. A comparison among the various ECP's used in the present work suggests that the SDD is comparable with LanL2DZ, with CEP-121, CEP-31, and SDDAll lying lower in accuracy. The bond dissociation energies calculated with the B3P86 functional in conjunction with LanL2DZ++G(2df,p), SDD++G(2df,p), CEP-121++G(2df,p), and CEP-31++G(2df,p) basis sets possess RMS deviations lying within a range of ca. 4 kJ mol⁻¹, while the B3P86/SDDAll++G(2df,p) level

performs rather poorly, with a higher RMS deviation of 13.9 kJ mol⁻¹. The relatively successful performance of the augmented variants of the small 3-21G basis set in conjunction with the B3P86 functional is worth noted, since this corresponds to a computer-effective means of achieving significant accuracy in large molecules. Tighter SCF convergence criteria (RMS density matrix to 10⁻⁸, MAX density matrix to 10⁻⁶) imposed in calculations employing DFT methods with basis sets containing diffusion functions (denoted in Table 2 by prefixing the basis set notation with the symbol SCFT-) do not lead to any improvement over those using normal convergence criteria (RMS density matrix to 10⁻⁴, MAX density matrix to 10⁻²). Thus, the use of the normal (and less expensive) criteria is sufficient in achieving the desired accuracy. Sophisticated post-SCF electron-correlation methods (CCSD(T), QCISD(T)) systematically underestimate the bond dissociation energies, an

TABLE 3: Root Mean Square Deviation (RMS), Mean Absolute Deviation (MAD), Average Deviation (AVD), Maximum Negative and Positive Deviations (MND, MPD), and Basis Set Superposition Error (BSSE) at Some Specific Levels of Theory for the Bond Dissociation Energies at 298.15 K of All Benchmark Species

level of theory	RMS	MAD	AVD	MND	MPD	BSSE
BHandH/AUG-cc-pVTZ_I/6-311+G(3df)	14.0	11.2	4.5	-27.9	24.9	-1.4
BHandH/cc-pVTZ	14.2	11.4	3.2	-33.3	24.1	-1.0
BHandH/AUG-cc-pVTZ	14.2	11.5	4.3	-35.0	24.9	-1.1
BHandH/6-311++G(2df,p)	14.2	11.1	2.6	-33.8	22.6	-2.1
B3PW91/SCFT-6-311++G(3df,2p)	14.3	13.2	-13.2	-31.7	-6.2	-2.5
B3P86/LanL2DZ++G(2d,p)	14.5	10.0	-8.3	-36.6	9.0	-1.7
B3PW91/cc-pVTZ	14.6	13.0	-12.7	-37.4	3.3	-0.01
B3PW91/AUG-cc-pVTZ_I/6-311+G(3df)	14.7	13.4	-13.4	-36.2	-7.3	-1.4
B3PW91/AUG-cc-pVTZ	14.8	13.4	-13.4	-42.2	-5.4	-1.0
B3PW91/6-311++G(3df,3pd)	15.1	13.6	-13.6	-37.7	-7.0	-2.7
B3PW91/6-311++G(2df,p)	15.1	14.1	-14.1	-32.9	-7.8	-1.9
G2	15.5	12.4	-11.6	-33.3	5.7	-8.3
B3LYP/6-311++G(3df,2p)	16.2	14.7	-14.5	-26.7	2.1	-1.5
B3P86/SVP_I/6-311G(d)	17.6	12.5	-11.5	-54.5	3.3	-4.0
B3LYP/AUG-cc-pVTZ_I/6-311+G(3df)	17.7	15.6	-15.4	-33.0	2.1	-1.3
B3LYP/6-311++G(2df,p)	17.7	16.2	-16.2	-29.0	0.9	-1.4
B3LYP/6-311++G(3df,3pd)	17.8	15.8	-15.6	-34.9	2.1	-2.5
B3LYP/AUG-cc-pVTZ	17.9	15.7	-15.5	-40.6	2.1	-1.0
B3LYP/cc-pVTZ	18.0	16.0	-15.7	-34.5	2.5	-1.2
B3LYP/AUG-cc-pV5Z_I/6-311+G(3df)	20.4	16.6	-16.4	-46.6	2.9	-4.4
B3P86/cc-pVDZ_I/6-311G(d)	20.9	14.6	-14.1	-66.0	3.3	-3.8
B3LYP/AUG-cc-pVQZ_I/6-311+G(3df)	20.9	17.3	-17.0	-47.4	2.8	-4.2
B3P86/6-311G(d)	22.7	16.7	-16.3	-55.2	3.0	-2.4
CCSD(T)/LanL2DZ++G(3d2f,2pd)	24.9	21.9	-21.9	-44.3	-4.3	-12.3
B3P86/LanL2DZG(d)	25.3	19.8	-17.5	-60.9	11.4	-2.7
QCISD(T)/6-311+G(3df,2p)	25.8	23.7	-23.7	-45.5	-6.5	-8.3
CCSD(T)/6-311++G(2df,pd)	29.4	26.7	-26.7	-55.0	-6.3	-10.1
CCSD(T)/LanL2DZ++G(2df,p)	33.4	31.3	-31.3	-52.8	-12.9	-9.8
B3P86/3-21G*	37.1	21.1	-17.6	-111.3	12.2	-20.2

effect which can be attributed to deficiencies of the basis sets employed. At the same time, these calculations possess large basis set superposition errors due to basis sets truncation effects. Even if the bond dissociation energies calculated by the QCISD(T)/6-311+G(3df,2p), CCSD(T)/6-311++G(2df,pd) and CCSD(T)/LanL2DZ++G(2df,p) levels of theory are not corrected for BSSE (ca. 9 kJ mol⁻¹), they still underestimate the experimental values by an average of ca. 16 kJ mol⁻¹. However, the efficiency of BSSE corrections in compensating for basis set deficiencies has been questioned.^{69,70} On the other hand, in calculations employing DFT methods, basis set superposition errors are inherently small (ca. 2 kJ mol⁻¹), and in most cases, they can be safely neglected, with the exception of the variants of the small 3-21G basis set. Apparently, in calculations involving DFT functionals, the saturation of the basis set can be attained at an earlier stage, indicated by the fast convergence of the B3P86 bond dissociation energies toward the experimental values for basis sets ranging from the small 3-21++G(2df,p) to the almost complete and very expensive AUG-cc-pV5Z_I/6-311+G(3df) basis set.

A comparison among all electron correlation methods employed in this study for the calculation of bond dissociation energies is presented in Table 4 in the order of increasing RMS deviation, averaged for all basis sets employed with each method. The B3P86 functional is clearly the most accurate for the calculation of bond dissociation energies, differing in RMS deviation by 3 and 5 kJ mol⁻¹ from its closest competitors, G2 theory and the BHandH functional, respectively. The higher accuracy of B3P86 and BHandH functionals in bond dissociation energies calculations constitutes another manifestation of the superior performance of hybrid functionals.⁵⁷ At the other end, functionals involving only local exchange terms (HFS, HFB, and XAlpha)^{23,24,71} or functionals involving the Slater or X α local exchange functionals^{62,71} perform disastrously with deviations exceeding 100 kJ mol⁻¹. Of the non-DFT methods and

apart from G2 theory, the MP2 method possesses the lowest deviations from the experimental bond dissociation energies, surpassing spin-projected MP2 (PMP2) and all higher order perturbation methods in accuracy, which tend to decrease the calculated bond dissociation energies as the treatment of electron correlation is improving, in accordance with the results of a recent study.²⁰ It must also be noted that the accuracy of G2 theory is greatly enhanced by the empirical corrections applied to the QCISD(T)/6-311+G(3df,2p) level of theory, which lower the RMS deviation from 25.8 kJ mol⁻¹ to 15.5 kJ mol⁻¹.

Detailed results for the bond dissociation energies calculated using the two most accurate levels of theory, B3P86/6-311++G(2df,p) and B3P86/6-311++G(3df,2p), are presented in Table 5. It should be noted that the calculated bond dissociation energy of IF appears to be underestimated, and this occurs systematically for almost all levels of theory employed in this study, indicating that the reported formation enthalpy of -94.8 ± 4.0 kJ mol⁻¹ for IF¹⁰ is probably in error. The above suggestion is supported by preliminary calculations at the presumably more accurate CCSD(T)/cc-pV5Z and CCSD(T)/AUG-cc-pV5Z levels of theory, which also presented large deviations on the order of 20 kJ mol⁻¹ for the enthalpy of formation for IF and the I-F bond dissociation energy.⁷²

In a recent work, the B3P86 functional has been also shown to reproduce experimental bond dissociation energies quite accurately for a set of 30 molecules containing X-X and X-Y bonds (X and Y = C, N, O, S, F, Cl, and Br) with an MAD of ca. 9 kJ mol⁻¹.⁷³ In addition, the B3P86 functional has been shown to be superior to MP2 and HF methods in the calculation of structural parameters, vibrational frequencies, and molecular polarizabilities for a set of 21 sulfur-containing molecules.⁷⁴

The dependence of the accuracy of the calculated bond dissociation energies on the geometry optimization method was also examined by reoptimizing the parent molecules and all radicals at various levels of theory, employing the HF, MP2,

TABLE 4: Number of Different Basis Sets Employed for Each Particular Electron Correlation Method and the Corresponding Root Mean Square Deviation (RMS), Mean Absolute Deviation (MAD), Average Deviation (AVD), Maximum Negative and Positive Deviations (MND, MPD), and Basis Set Superposition Error (BSSE) for the Calculated Bond Dissociation Energies of All Benchmark Species

electron correlation method	no. of basis sets	RMS	MAD	AVD	MND	MPD	BSSE
B3P86	37	12.4	7.8	-4.3	-111.3	19.4	-2.9
G2	-	15.5	12.4	-11.6	-33.3	5.7	-8.3
BHandH	33	17.4	12.4	-1.2	-118.5	29.0	-3.2
G96PW91	7	17.7	14.5	-2.9	-47.1	37.7	-4.5
PW91VWN	9	18.3	13.8	1.3	-38.2	48.3	-3.0
PW91VWN5	9	18.7	15.0	-5.0	-43.5	39.8	-2.1
MP2	4	19.0	16.4	-15.7	-38.9	11.2	-9.6
BP86	32	19.1	13.1	5.6	-107.0	73.7	-2.6
PW91PL	9	19.7	14.8	-1.4	-41.4	79.5	-2.6
MPWVWN	8	19.7	15.5	-4.8	-43.5	65.4	-2.9
G96P86	32	20.2	14.6	7.7	-438.6	59.7	-3.6
B3PW91	36	20.8	17.5	-17.4	-128.6	47.0	-3.2
BLYP	31	21.8	17.9	-10.7	-321.6	75.7	-2.9
BPW91	7	22.0	17.8	-1.7	-46.1	79.3	-2.8
MPWLYP	29	22.6	17.1	-3.5	-375.5	81.9	-2.5
MPWVWN5	8	23.0	18.9	-9.9	-48.8	58.8	-1.1
G96LYP	29	23.3	18.5	-10.5	-375.5	281.0	-3.9
MPWPL	8	23.7	16.8	-7.8	-124.5	39.0	-2.1
PW91LYP	29	23.7	16.8	1.9	-375.5	98.1	-3.1
B3LYP	37	24.1	20.2	-20.0	-131.1	12.2	-3.2
MPWPW91	7	24.5	19.2	3.3	-41.8	88.9	-0.6
G96VWN	7	25.1	20.9	-14.4	-53.7	34.8	-3.9
MPW1PW91	30	25.4	22.1	-22.1	-135.2	-7.7	-3.4
BVWN	21	25.4	20.1	-13.2	-114.2	59.6	-3.1
PMP2	4	25.6	23.4	-23.4	-48.0	1.7	-9.7
MPWP86	29	25.8	18.2	13.3	-120.4	104.5	-1.6
QCISD(T)	1	25.8	23.7	-23.7	-45.5	-6.5	-8.3
PW91PW91	9	26.0	20.6	8.0	-36.9	69.9	-0.9
BPL	21	26.9	21.5	-16.2	-375.5	41.0	-3.2
G96PL	7	27.9	23.4	-18.2	-58.1	35.1	-4.2
CCSD(T)	3	29.4	26.6	-26.6	-55.0	-4.3	-10.7
BVWN5	21	29.6	23.9	-20.0	-119.9	41.7	-3.7
G96VWN5	7	31.0	26.1	-22.1	-61.5	35.7	-3.4
PW91P86	32	31.5	22.2	19.1	-117.2	114.5	-2.2
B1LYP	15	33.6	30.6	-30.6	-84.9	6.8	-3.0
MP4SDQ	4	37.3	33.3	-33.3	-65.6	-4.6	-9.5
QCISD	1	37.8	34.1	-34.1	-62.2	-8.8	-7.8
CCSD	3	40.5	36.4	-36.4	-72.5	-4.3	-10.0
BHandHLYP	33	54.0	41.1	-41.1	-158.0	4.3	-3.1
HFS	20	56.2	41.1	-9.1	-177.3	118.6	-4.2
XAlpha	20	56.9	41.8	0.6	-152.9	134.6	-4.1
SVWN5	17	78.3	53.0	52.6	-60.4	164.6	-5.3
SVWN	17	84.7	56.5	56.1	-54.3	171.7	-5.3
SLYP	17	93.4	47.6	44.3	-70.9	218.5	-5.5
XAVWN	17	94.7	59.1	58.9	-30.4	187.0	-4.9
SPW91	7	98.5	40.9	35.6	-38.5	194.3	-4.9
HFB	20	100.9	81.3	-81.3	-232.1	-23.1	-3.6
XALYP	17	103.8	47.2	44.4	-45.4	197.9	-4.7
XAPW91	7	106.3	45.9	41.0	-32.5	209.3	-4.6
SP86	17	107.4	47.9	45.3	-46.4	204.0	-4.2

and MP2(FULL) methods and the B3LYP and B3P86 functionals with several small basis sets, namely, 3-21G*, 6-31G(d), 6-311G(d), and 6-311+G(d). The 6-31G(d) basis set was extended by using the small SV4P basis set for iodine,⁷⁵ denoted as 6-31G(d)_I/SV4P. The vibrational frequencies and the corresponding scaling factors were also calculated for each optimization level, with the exception of the MP2(FULL)/6-31G(d) level, where the MP2/6-311G(d) frequencies with a scaling factor of 0.9872 were used instead. Subsequently, single-point calculations at the B3P86/6-311++G(2df,p) and B3P86/6-311++G(3df,2p) levels were performed, and the bond dissociation energies were derived by ignoring the small basis

TABLE 5: Deviations from the Experimental Values and BSSE Corrections (in kJ mol⁻¹) for Each Particular Bond Dissociation Energy at 298.15 K at the Two Most Accurate Levels of Theory, B3P86/6-311++G(2df,p) and B3P86/6-311++G(3df,2p)

bond	experimental value ^a	B3P86/6-311++G(2df,p)		B3P86/6-311++G(3df,2p)	
		deviation	BSSE	deviation	BSSE
H-H	436.0 ± 0.01	8.6	-0.007	9.7	-0.01
F-F	158.8 ± 0.4	-1.5	-3.0	-2.5	-3.3
Cl-Cl	242.6 ± 0.01	-0.8	-3.4	-1.1	-4.4
Br-Br	192.8 ± 0.2	-0.8	-2.7	3.0	0.0
I-I	151.1 ± 0.1	-6.8	-3.8	-6.3	-5.2
CH ₃ -H	438.6 ± 1.1	1.7	-0.4	2.5	-0.5
H-F	569.9 ± 0.8	0.4	-1.4	5.1	-1.8
CH ₂ F-H	418.8 ± 9.8	3.0	-0.6	2.8	-0.8
CH ₃ -F	459.4 ± 5.1	1.5	-3.2	3.5	-4.0
H-Cl	431.6 ± 0.1	2.9	-1.4	7.3	-1.8
Cl-F	251.0 ± 4.0	3.4	-3.5	7.4	-4.3
CH ₂ Cl-H	423.0 ± 4.3	-8.7	-0.8	-8.9	-2.0
CH ₃ -Cl	350.7 ± 1.2	-4.5	-3.0	-3.0	-3.4
H-Br	366.3 ± 0.2	4.5	-0.9	6.8	-0.4
Br-F	249.7 ± 4.0	-1.9	-2.9	2.4	-1.6
Br-Cl	218.5 ± 4.0	0.3	-2.6	2.2	-1.9
CH ₂ Br-H	419.7 ± 4.3	-0.2	-0.7	0.6	-0.6
CH ₃ -Br	291.9 ± 1.3	-2.8	-2.1	-0.9	-0.5
H-I	298.4 ± 0.1	6.2	-1.6	7.3	-1.4
I-F	280.9 ± 4.0	-20.1	-3.9	-17.6	-4.2
I-Cl	210.6 ± 4.0	-4.7	-3.2	-4.2	-4.4
CH ₂ I-H	421.3 ± 6.8	-1.8	-0.8	0.1	-0.7
CH ₃ -I	238.2 ± 1.7	-5.4	-3.1	-5.2	-3.6

^a Obtained from the corresponding formation enthalpies from ref 11, except those for halomethyl radicals are from ref 6, and those for CH₃Br and CH₃I are from refs 21 and 22, respectively.

sets superposition errors (ca. 2 kJ mol⁻¹). The results are presented in Table 6 for each geometry optimization level. The best agreement of the calculated structural parameters with the experimental ones (for 21 species, containing all stable molecules and including CH₃ and CH₂Br radicals) is consistently exhibited by the B3P86 functional, followed by those employing the MP2 method. Furthermore, the structural parameters calculated by using the B3P86 functional appear to be closer to the experimental ones than those obtained by the commonly used B3LYP functional.^{57,76} In the case of the MP2(FULL)/6-31G(d)_I/SV4P level, the calculated structures are slightly closer to the experimental ones than those derived by the MP2/6-31G(d)_I/SV4P level, indicating that no significant improvement in the structures is achieved by using the costly correlation of all electrons by the MP2(FULL) method. Larger basis sets tend to improve the calculated structures, with the closest agreement presented by the LanL2DZ ECP, augmented by a set of d- polarization functions on all heavy atoms (denoted as LanL2DZG(d)). Therefore, the geometry optimization at the B3P86/LanL2DZG(d) level of theory, combines the computational efficiency for application to large halogen-containing species with sufficient accuracy in reproducing the experimental structural parameters. Regarding the calculation of vibrational frequencies, the B3LYP functional approaches the experimental values quite closely, while the worst performance is presented by the HF/6-31G(d)_I/SV4P level of theory. Finally, the dependence of the calculated bond dissociation energies on the level chosen for the geometry optimization step was found to be very weak, with RMS deviations differing from each other by ca. 1 kJ mol⁻¹.

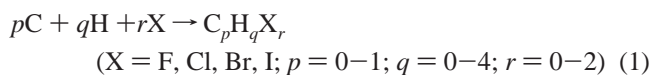
In addition to bond dissociation energy which is greatly correlated with molecular reactivity, the enthalpy of formation constitutes another significant quantity, being extensively used

TABLE 6: Dependence of the Accuracy (Expressed as the RMS Deviation from Experimental Values) on the Molecular Geometry Optimization Level for the Bond Dissociation Energies Calculated at the B3P86/6-311++G(2df,p) and B3P86/6-311++G(3df,2p) Levels of Theory^a

optimization level	% deviation of structural parameter values	vibrational scale factor	bond dissociation energy deviations (RMS)	
			B3P86/ 6-311++G(2df,p)	B3P86/ 6-311++G(3df,2p)
B3LYP/3-21Gs	1.79	0.9903	5.5	6.0
B3P86/3-21Gs	1.36	0.9703	5.3	6.0
MP2/3-21Gs	1.72	0.9609	5.6	6.1
HF/6-31G(d)_I/SV4P	1.58	0.9102	5.6	6.2
B3P86/6-31G(d)_I/SV4P	1.24	0.9723	5.8	6.7
MP2/6-31G(d)_I/SV4P	1.57	0.9661	5.7	6.5
MP2(FULL)/6-31G(d)_I/SV4P	1.54	0.9872 ^b	5.7	6.5
B3LYP/LanL2DZG(d)	1.49	1.0049	5.4	6.2
B3P86/LanL2DZG(d)	1.10	0.9847	5.4	6.3
MP2/LanL2DZG(d)	1.34	0.9829	5.3	6.2
B3LYP/6-311G(d)	1.62	1.0090	5.7	6.4
B3P86/6-311G(d)	1.11	0.9865	5.5	6.4
MP2/6-311G(d)	1.35	0.9872	5.6	6.3
MP2/6-311+G(d)	1.35	0.9882	5.6	6.3

^a The deviations of the calculated structural parameter values (bond lengths, bond angles, and dihedral angles) from the experimental values (averaged for all species) and the corresponding vibrational scale factors evaluated for each optimization level are also listed. ^b The vibrational frequencies calculated at the MP2/6-311G(d) level were employed for the zero-point energies and thermal energy corrections at the MP2(FULL)/6-31G(d)_I/SV4P level geometry optimization.

in the assessment of the accuracy of thermochemical calculations. Therefore, the enthalpies of formation of all species employed in this study at 298.15 K were also calculated by using the reverse atomization reaction



The structural parameters and the vibrational frequencies calculated at the MP2/6-311G(d) level of theory were also used. The zero-point energies and thermal corrections to the enthalpy (scaling down the vibrational frequencies by 0.9872) were added to the absolute electronic energies derived by single-point energy calculations at more than 800 levels of theory to obtain the absolute enthalpies at 298.15 K. The absolute electronic energies of carbon and halogen atoms were appropriately lowered by taking into account the spin-orbit splitting of their ³P and ²P states, respectively. The enthalpies of formation of the 24 benchmark species of this study for the levels of theory presenting RMS deviations lower than 14 kJ mol⁻¹ are presented in Table 7. In addition, selected results at interesting but less accurate levels of theory are listed in Table 8. An examination of the results in Table 7 indicates that G2 constitutes a fairly accurate level of theory for the calculation of formation enthalpies, followed by various combinations of the B3PW91 and B3LYP functionals with a variety of large basis sets. The result is in accordance with previous studies, which indicated the superiority of the B3LYP and B3PW91 functionals in calculations of the formation enthalpies for much larger samples of species.^{15-19,57,76,77} From the results in Table 8, it can be noted that the B3P86 functional overbinds all molecules, leading to significantly underestimated enthalpies of formation, as found in earlier studies.¹⁷ The trends in accuracy as a function of either a particular functional or a basis set are less clear, with various combinations of functionals with basis sets producing results of comparable accuracy. However, large basis sets tend to improve the calculated values, with the notable exception of the small 3-21++G(3df,2p) basis set in combination with the B3LYP, BVWN, B3PW91, and BPL functionals. By taking into account the equally good performance of the B3P86/3-21G++G(3df,2p) level in the bond dissociation energy calculations, the success of the small 3-21++G(3df,2p) basis set may indicate that in thermochemical calculations using DFT functionals, the

size of the basis set is comparable in importance with the presence of polarization and diffusion functions.^{57,68} Particular attention should also be paid to the B3PW91/AUG-cc-pVQZ_I/6-311+G(3df) and B3PW91/AUG-cc-pV5Z_I/6-311+G(3df) levels of theory, which are sufficiently accurate in both thermochemical properties calculations (bond dissociation energies and enthalpies of formation; see Tables 2 and 7). The latter finding may indicate the reliability of the combination of the B3PW91 functional with highly extended correlation-consistent basis sets in thermochemical calculations, although the size of these basis sets places some constraints due to the increased computational cost for larger species. The overall performance of all electron-correlation methods for the calculation of the enthalpies of formation is presented in Table 9. Thus, G2 theory constitutes the most accurate level of theory of all examined in this study, mostly favored by the empirical corrections which lower the RMS deviation from 28.9 kJ mol⁻¹ for the QCISD-(T)/6-311+G(3df,2p) level to 8.7 kJ mol⁻¹ for G2. Regarding the DFT methods, B3PW91 constitutes the most accurate functional, deviating on the average almost 5 kJ mol⁻¹ less than B3LYP. In recent studies on the efficiency of G2 theory and DFT methods for the calculation of enthalpies of formation in large samples of molecules (referred to as "G2 neutral test set"), B3LYP and B3PW91 functionals were found to be of comparable accuracy, with a slight superiority of B3LYP.^{17,19} Therefore, the inversion noted in this study may be considered incidental due to the limited number of species involved. All DFT functionals involving Slater of X α exchange overbind all molecules significantly, as has been already reported,^{57,17} and thus, they are totally unsuitable for thermochemical calculations. On the other hand, post-SCF methods, in combination with relatively small basis sets, overestimate the enthalpies of formation, with accuracy inversely dependent on the complexity of the electron-correlation method. However, the accuracy of these methods in thermochemical calculations has been shown to be greatly improved with very large basis sets or extended correlation-consistent basis sets, aided by extrapolations in reaching an effectively complete basis set limit.^{20,78-80} The deviations from the experimental values for the calculated enthalpies of formation of the 24 benchmark molecules of this study are listed in Table 10 for three most successful levels of theory, namely, G2, B3PW91/6-311++G(3df,2p) and B3PW91/

TABLE 7: Root Mean Square Deviation (RMS), Mean Absolute Deviation (MAD), Average Deviation (AVD), and Maximum Negative and Positive Deviations (MND, MPD) at Levels of Theory Possessing an RMS Deviation Less than 14 kJ mol⁻¹ for the Enthalpies of Formation at 298.15 K for All Benchmark Species

level of theory	RMS	MAD	AVD	MND	MPD
G2	8.8	7.4	7.2	-3.0	19.3
B3LYP/3-21++G(3df,2p)	9.3	7.8	5.0	-6.9	19.4
B3PW91/6-311++G(3df,2p)	9.8	8.4	4.5	-17.1	26.3
B3PW91/AUG-cc-pV5Z_I/6-311+G(3df)	10.1	8.3	3.3	-16.6	28.4
B3PW91/SCFT-6-311++G(3df,2p)	10.1	8.6	4.8	-17.3	27.6
B3PW91/AUG-cc-pVQZ_I/6-311+G(3df)	10.4	8.7	4.4	-14.3	30.3
BVWN/3-21++G(3df,2p)	10.8	8.2	-3.5	-27.4	11.9
B3PW91/6-311++G(3df,3pd)	11.0	8.8	4.5	-18.6	33.5
B3PW91/6-311++G(2df,p)	11.0	9.7	7.2	-12.7	29.1
B3PW91/AUG-cc-pVTZ_I/6-311+G(3df)	11.0	9.5	6.4	-10.8	32.8
B3PW91/AUG-cc-pVTZ_I/6-311+G(2df)	11.1	9.6	6.4	-10.8	32.3
PW91PL/SDDAll++G(3d2f,2pd)	11.4	8.9	-0.8	-29.8	18.6
B3PW91/SCFT-6-311++G(2df,p)	11.4	10.0	7.6	-12.8	30.4
B3LYP/AUG-cc-pV5Z_I/6-311+G(3df)	11.4	9.2	7.2	-8.5	25.3
B3PW91/AUG-cc-pVTZ	11.6	9.8	6.9	-10.8	39.6
B3PW91/3-21++G(3df,2p)	11.7	9.8	1.0	-19.7	25.1
PW91VWN/SDDAll++G(2df,p)	11.8	9.0	-2.1	-27.8	20.3
B3PW91/cc-pVTZ	11.9	10.0	7.4	-10.8	34.6
BPL/3-21++G(3df,2p)	12.2	9.7	2.7	-26.9	21.7
B3LYP/AUG-cc-pVQZ_I/6-311+G(3df)	12.4	9.8	8.3	-8.3	27.2
BPL/6-311++G(2df,p)	12.4	9.9	0.3	-30.0	19.5
B3LYP/6-311++G(3df,2p)	12.5	10.5	9.2	-6.3	25.0
B3LYP/SCFT-6-311++G(3df,2p)	12.5	10.5	9.2	-6.3	24.9
PW91PL/SDDAll++G(2df,p)	12.6	10.2	3.8	-27.3	24.2
BPL/6-311++G(3df,2p)	12.6	10.3	-2.6	-31.1	17.7
MPWVWN/SDDAll++G(3d2f,2pd)	12.7	9.9	2.3	-31.3	24.1
B3PW91/LanL2DZ++G(3d2f,2pd)	12.7	11.1	8.0	-16.0	29.8
MPWVWN5/6-311++G(2df,p)	12.7	10.1	-3.7	-29.3	17.5
B3PW91/LanL2DZ++G(3d2f,2p)	12.8	11.2	8.3	-15.5	29.8
G96VWN/6-311++G(2df,p)	12.8	10.0	-1.3	-32.4	20.1
B3PW91/LanL2DZ++G(3df,2pd)	12.8	11.2	8.2	-15.8	29.6
G96LYP/6-311++G(2df,p)	12.8	9.3	-1.7	-35.7	18.0
B3PW91/LanL2DZ-OPT(++G(3d2f,2pd))	12.9	11.3	8.5	-15.1	29.5
B3LYP/6-311++G(3df,3pd)	13.0	10.5	8.8	-7.7	31.0
PW91VWN/SDDAll++G(3d2f,2pd)	13.3	10.6	-6.8	-30.2	14.7
BVWN5/6-311++G(3df,2p)	13.3	10.8	1.8	-31.7	22.6
PW91VWN5/SDDAll++G(3d2f,2pd)	13.3	10.7	4.1	-30.4	24.1
B3PW91/AUG-cc-pVTZ_I/6-311+G(d)	13.3	10.7	7.8	-10.8	39.6
B3PW91/LanL2DZ++G(3d2f,p)	13.7	12.0	10.6	-12.0	29.8
B3PW91/SDD++G(3d2f,2pd)	13.7	11.1	8.4	-15.2	40.4
G96PL/6-311++G(2df,p)	13.9	12.5	8.5	-12.2	22.8
G96P86/CEP-31++G(2df,p)	14.0	12.3	-6.1	-19.6	19.3
B3LYP/AUG-cc-pVTZ_I/6-311+G(3df)	14.0	11.4	10.7	-6.3	29.8

TABLE 8: Root Mean Square Deviation (RMS), Mean Absolute Deviation (MAD), Average Deviation (AVD), and Maximum Negative and Positive Deviations (MND, MPD) at Some Specific Levels of Theory for the Enthalpies of Formation at 298.15 K for All Benchmark Species

level of theory	RMS	MAD	AVD	MND	MPD
B3LYP/AUG-cc-pVTZ_I/6-311+G(3df)	14.0	11.4	10.7	-6.3	29.8
B3LYP/6-311++G(2df,p)	14.5	12.5	12.2	-3.1	27.6
B3PW91/6-311++G(2d,p)	15.7	13.3	12.4	-8.4	40.5
CCSD(T)/LanL2DZ++G(3d2f,2pd)	18.9	16.9	16.9	0.2	29.5
B3P86/SDDAll++G(3d2f,2pd)	24.6	19.8	-10.1	-43.2	37.8
B3P86/6-311G(d)	26.1	23.7	2.2	-31.5	50.5
B3P86/6-311++G(2d,p)	28.2	22.2	-14.8	-47.0	28.1
QCISD(T)/6-311+G(3df,2p)	29.0	26.9	26.9	9.2	47.4
B3P86/6-311++G(2df,p)	30.0	22.0	-20.2	-51.5	16.3
CCSD(T)/6-311++G(2df,p)	30.4	28.1	28.1	4.1	48.4
B3P86/LanL2DZ++G(3df,2pd)	31.3	24.0	-19.4	-54.9	16.0
B3P86/LanL2DZ++G(3d2f,2pd)	31.4	24.0	-19.5	-55.0	16.0
B3P86/3-21++G(3df,2p)	31.7	26.2	-26.2	-58.6	0.3
B3P86/6-311++G(3df,2p)	32.6	24.3	-23.0	-56.3	13.6
B3P86/AUG-cc-pVQZ_I/6-311+G(3df)	33.4	25.1	-23.1	-54.2	17.6
B3P86/AUG-cc-pV5Z_I/6-311+G(3df)	34.1	25.8	-24.1	-55.6	15.8
CCSD(T)/LanL2DZ++G(2df,p)	44.5	40.5	40.5	15.1	69.8

AUG-cc-pV5Z_I/6-311+G(3df). Iodine monofluoride IF deviates significantly, which may be attributed to an erroneous value for its experimental enthalpy of formation, as has been already discussed.

The widely different behavior of the B3P86 functional in the calculations of bond dissociation energies and enthalpies of formation is striking and deserves a closer examination. The

enthalpy of formation of a species, as described and calculated by eq 1, can be expanded in a number of consecutive bond fission steps, and each bond dissociation energy can be separately calculated. Therefore, the geometries of all intermediate radical species CH_mX_n (X = F, Cl, Br, and I; m = 0-3; n = 0,1) were optimized at the MP2/6-311G(d) level, and their vibrational frequencies were calculated and scaled by 0.9872.

TABLE 9: Number of Different Basis Sets Employed for Each Particular Electron Correlation Method and the Corresponding Root Mean Square Deviation (RMS), Mean Absolute Deviation (MAD), Average Deviation (AVD), and Maximum Negative and Positive Deviations (MND, MPD) for the Enthalpies of Formation at 298.15 K for All Benchmark Species

electron correlation method	no. of basis sets	RMS	MAD	AVD	MND	MPD
G2	—	8.8	7.4	7.2	-3.0	19.3
B3PW91	36	18.8	14.6	10.4	-65.1	115.7
MPWVWN5	8	21.2	16.8	1.0	-63.1	47.2
BVWN	21	21.5	16.7	2.0	-90.7	99.7
MPWPL	8	21.5	16.5	-2.9	-67.3	73.4
G96VWN	7	22.3	17.5	2.9	-61.3	55.7
BPL	21	22.8	17.8	8.4	-61.3	375.0
B3LYP	37	23.0	17.9	15.9	-56.0	116.8
PW91VWN5	9	23.3	18.4	-9.4	-71.3	41.8
G96PL	7	23.7	18.9	8.6	-45.1	66.5
MPW1PW91	30	23.9	19.6	17.1	-63.9	122.3
MPWVWN	8	24.3	18.8	-10.5	-73.9	41.9
G96PW91	7	24.8	18.9	-2.3	-91.0	46.1
BVWN5	21	24.9	19.9	12.3	-55.5	105.1
MPWLYP	29	25.0	17.7	-1.7	-99.6	375.0
BLYP	31	25.0	18.6	8.6	-87.4	321.7
BPW91	7	25.4	19.1	-7.3	-94.9	42.3
PW91PL	9	26.6	20.6	-14.5	-81.3	39.8
MP2	4	26.6	20.6	19.0	-13.6	83.4
G96LYP	29	26.7	20.1	9.8	-76.6	375.0
G96VWN5	7	26.9	22.0	13.6	-54.2	63.2
PW91LYP	29	28.1	20.6	-11.8	-110.8	375.0
G96P86	32	28.3	22.8	-20.1	-97.4	436.0
QCISD(T)	1	29.0	26.9	26.9	9.2	47.4
PMP2	4	30.4	25.2	24.9	-8.4	86.9
B3P86	37	30.8	23.6	-16.5	-90.6	98.5
PW91VWN	9	31.5	24.7	-20.8	-84.8	36.6
MPWPW91	7	31.7	21.9	-13.2	-115.9	39.3
CCSD(T)	3	33.0	28.5	28.5	0.2	69.8
BP86	32	33.0	26.6	-24.9	-116.7	92.8
PW91PW91	9	34.2	26.7	-22.3	-108.7	36.0
BHandH	33	38.5	29.2	-18.6	-107.8	105.8
B1LYP	15	39.0	34.5	33.7	-46.0	95.4
MP4SDQ	4	42.1	38.7	38.7	5.2	80.4
QCISD	1	43.9	41.3	41.3	9.2	66.7
MPWP86	29	44.5	37.0	-36.0	-141.5	68.8
CCSD	3	46.5	42.4	42.4	3.8	86.8
PW91P86	32	56.6	45.9	-45.4	-150.8	65.8
BHandHLYP	33	57.4	48.3	48.2	-27.3	145.3
XAlpha	20	73.9	43.2	4.5	-148.2	212.4
HFS	20	87.0	46.1	8.0	-145.7	262.3
HFB	20	89.8	77.6	77.5	-6.9	415.3
XAVWN	17	115.0	61.6	-61.6	-349.0	-0.2
SVWN	17	119.0	60.9	-60.6	-301.1	21.1
SVWN5	17	122.1	59.9	-59.5	-280.3	26.9
SPW91	7	122.1	55.2	-45.3	-271.5	38.5
XAPW91	7	123.4	55.8	-45.6	-338.7	32.5
SP86	17	124.5	61.6	-57.5	-349.1	20.4
SLYP	17	124.5	59.1	-53.4	-298.2	32.8
XALYP	17	124.6	57.1	-52.1	-339.9	25.2

Furthermore, single-point energy calculations at levels of theory leading to the most accurate enthalpies of formation and bond dissociation energies for stable species were performed. Thus, the bond dissociation energies at 298.15 K of all intermediate species were calculated at the G2, B3PW91/6-311++G(3df,2p), and B3P86/6-311++G(2df,p) levels of theory. Furthermore, they were corrected for BSSE and the spin-orbit splitting of carbon and halogen atoms as well as for the spin-orbit splitting of the $^2\Pi$ state of the diatomic species CH (27.95 cm^{-1}), CF (77.12 cm^{-1}), and CBr (466 cm^{-1}).⁸¹ For CHF, CHCl, and CHBr, the singlet states were found to be energetically lower than the triplet states (by 71.3, 34.9, and 32.2 kJ mol^{-1} , respectively, at the G2 level), in accordance with experimental

TABLE 10: Deviations from the Experimental Values (in kJ mol^{-1}) for Each Particular Enthalpy of Formation at 298.15 K at Three Selected Levels of Theory: G2, B3PW91/6-311++G(3df,2p), and B3PW91/AUG-cc-pV5Z_I/6-311+G(3df)

species	experimental value ^a	G2	B3PW91/6-311++G(3df,2p)	B3PW91/AUG-cc-pV5Z_I/6-311+G(3df)
H ₂	0.0	-3.0	10.2	9.5
CH ₄	-74.9 ± 0.4	6.7	7.6	5.6
CH ₃	145.7 ± 1.0	8.6	-4.8	-6.4
F ₂	0.0	8.2	14.6	10.3
HF	-272.6 ± 0.7	0.5	12.1	12.1
CH ₃ F	-234.3 ± 5.0	2.2	2.4	3.9
CH ₂ F	-33.5 ± 8.4	10.6	-9.0	-7.1
Cl ₂	0.0	15.7	6.9	5.3
HCl	-92.3 ± 0.1	3.9	6.1	7.2
ClF	-50.3 ± 4.0	2.8	1.9	2.2
CH ₃ Cl	-83.7 ± 0.7	11.0	5.5	6.2
CH ₂ Cl	121.3 ± 4.2	7.4	-17.2	-16.6
Br ₂	30.9 ± 0.1	8.5	5.0	3.8
HBr	-36.4 ± 0.2	1.8	7.0	6.7
BrF	-58.5 ± 4.0	5.8	8.4	9.7
BrCl	14.6 ± 4.0	10.7	5.0	4.5
CH ₃ Br	-34.3 ± 0.8	5.4	5.1	3.4
CH ₂ Br	167.4 ± 4.2	10.0	-8.4	-10.0
I ₂	62.4 ± 0.1	10.9	8.8	11.4
HI	26.4 ± 0.1	0.6	5.6	-0.1
IF	-94.8 ± 4.0	19.3	26.3	28.4
ICl	17.5 ± 4.0	13.3	8.9	8.6
CH ₃ I	14.3 ± 1.4	4.2	6.2	-3.0
CH ₂ I	217.6 ± 6.7	7.2	-7.5	-16.4

^a Obtained from ref 11, except those for halomethyl radicals from ref 6, and CH₃Br and CH₃I, from refs 21 and 22, respectively.

results.^{82,83} The experimental bond dissociation energies were computed from the corresponding enthalpies of formation, obtained from NIST-JANAF Thermochemical tables,^{10,11} with the exception of halomethyl radicals⁶ and CHF.⁵⁸ The results for some of the intermediate species whose experimental bond dissociation energies can be inferred from the corresponding enthalpies of formation available are displayed in Table 11. Evidently, the B3P86 functional overestimates the bond dissociation energies of most species, consistently leading to stronger bonds. In contrast, G2 theory leads to bond dissociation energies with deviations from experimental values balanced on both negative and positive sides, resulting in a small total average deviation (AVD), in a similar manner with the B3PW91 functional. However, several large deviations can still be noted (especially for the CCl-H and C-Cl bond dissociation energies) from rather uncertain experimental values. Therefore, the superiority of G2 theory and B3PW91 functional (as well as that of B3LYP functional, whose behavior was found to be similar to B3PW91) in the calculation of enthalpies of formation is possibly due to the mutual cancellation of errors over the entire set of the intermediate reactions which constitute the formation of a molecule from the corresponding atoms.

Unfortunately, the success of the B3P86 functional in the calculation of the bond dissociation energies is apparently limited to those for only closed-shell species. However, regarding at least atmospheric chemistry, this limitation is not particularly severe, since the prediction of accurate bond dissociation energy for stable molecules is the starting point in the assessment of their atmospheric reactivity. Furthermore, the combination of the B3P86 functional with basis sets of moderate size augmented with diffusion and polarization functions constitutes a cost-effective level of theory which can be applied to large molecules, while the geometry optimization and vibrational frequencies calculation remain the most computer-intensive steps. In this direction, the calculation of bond

TABLE 11: Deviations from the Experimental Values for the Bond Dissociation Energies (in kJ mol⁻¹) at 298.15 K of the Radical Species of This Study, Calculated at the G2, B3PW91/6-311++G(3df,2p), and B3P86/6-311++G(2df,p) Levels of Theory

bond	experimental value ^a	deviation		
		G2	B3PW91/ 6-311++G(3df,2p)	B3P86/ 6-311++G(2df,p)
CH ₂ -H	458.7 ± 2.3	3.5	-3.7	12.9
CH-H	425.7 ± 4.5	-14.7	11.8	20.3
C-H	340.5 ± 4.0	-3.2	-4.7	10.5
CH ₂ -F	499.2 ± 8.7	-8.6	-3.3	11.2
CHF-H	414.5 ± 15.5	-30.5	-2.1	8.6
CH-F	510.5 ± 13.6	4.7	10.3	22.6
CF-H	310.2 ± 18.4	4.6	-9.9	4.4
C-F	540.8 ± 13.0	-2.6	15.3	28.5
CH ₂ -Cl	386.4 ± 4.7	-4.4	5.6	16.7
CHCl-H	431.4 ± 13.7	-21.4	4.2	15.1
CH-Cl	380.7 ± 13.6	11.9	12.0	21.3
CCl-H	385.4 ± 18.4	-56.4	-68.7	-54.4
C-Cl	335.9 ± 13.0	52.7	75.9	85.9
CH ₂ -Br	330.9 ± 4.7	-7.5	-0.5	10.2
C-Br	318.1 ± 13.0	3.1	24.9	34.6
CH ₂ -I	275.6 ± 7.0	-9.5	-4.5	8.2
total deviation				
RMS	-	22.4	27.3	30.5
MAD	-	14.9	16.1	22.8
AVD	-	-4.9	3.9	16.0
MND	-	-56.4	-68.7	-54.4
MPD	-	52.6	75.9	85.9
BSSE	-	-7.4	-2.0	-1.9

^a Obtained from ref 11, except those for halomethyl radicals are from ref 6, and those for CHF are from ref 58.

dissociation energies of a larger set of 60 bonds in 41 halogen-containing molecules (including the 19 benchmark molecules) was undertaken by using the reliable and computationally efficient B3P86/LanL2DZG(d) level of theory for the geometry optimization and vibrational frequencies calculation. The vibrational frequencies were scaled down by the factor 0.9847. The bond dissociation energies at 298.15 K were calculated at the B3P86/6-311++G(2df,p) level of theory (ignoring BSSE), and the results are shown in Table 12. The experimental bond dissociation energies were computed from the corresponding enthalpies of formation, obtained from the NIST-JANAF Thermochemical tables,^{10,11} with the exceptions of monohalomethyl radicals, CHF₂, CHCl₂, CHBr₂, CBr₃, CH₂Br₂, CF₃-CH₂, CF₃CF₂ and CF₃CH₃,⁶ CH₃Br,²¹ CH₃I,²² alkyl and vinyl radicals,⁸⁴ alkanes,⁸⁵ CH₂I₂ and Cl₄,⁸⁶ CHBr₃,⁸⁷ and CBr₄.⁸⁸

As can be seen in Table 12, the total RMS deviation of the calculated values is 12.7 kJ mol⁻¹, with a MAD of 9.1 kJ mol⁻¹, indicating that the B3P86/6-311++G(2df,p) level of theory remains sufficiently accurate for the larger set of molecules. However, bond dissociation energies are mostly underestimated, while particular deviations (excluding that for iodine monofluoride IF) tend to be larger for the heavier molecules of the set. This suggests that empirical corrections dependent on the total number of electrons would improve the accuracy of the calculated values. These corrections could be fit as to either lower the total electronic energy E_e of the closed-shell molecules or increase the total electronic energy of the open-shell radicals. Both kinds of empirical corrections were tested by systematically varying the factor γ multiplied by the total number of electrons N_e in order to minimize the RMS deviation. The decrease of the total electronic energy for all closed-shell molecules was optimal for $\gamma = 6 \times 10^{-5}$ Hartrees/electron, with a reduction of the RMS to 8.8 kJ mol⁻¹, while by applying the correction to molecules of three or more atoms, we obtained an optimal γ of 7×10^{-5} Hartrees/electron, with an even lower RMS of 7.9

kJ mol⁻¹. On the other hand, by increasing the total electronic energy of open-shell radicals (excluding atoms) by $\gamma = 9 \times 10^{-5}$ Hartrees/electron, we finally obtained an RMS deviation of 8.0 kJ mol⁻¹. Both kinds of correction were equally successful in improving the accuracy of the calculated values, reducing the overall errors by ca. 4 kJ mol⁻¹. Assuming that open-shell calculations are mainly responsible for the errors in DFT calculations, the increase of the total electronic energies of the radicals by $N_e \cdot 9 \times 10^{-5}$ Hartrees was considered to be more suitable, and the empirically corrected bond dissociation energies of all molecules considered in the present study are shown in Table 12 for the B3P86/6-311++G(2df,p) level of theory. Similarly, an empirical adjustment of the total electronic energy of the radicals by $N_e \cdot 8 \times 10^{-5}$ Hartrees was also found suitable to decrease the total RMS deviation from 12.7 to 9.8 kJ mol⁻¹ for the next successful level of theory, B3P86/6-311++G(3df,2p). Moreover, both levels of theory overestimate the HCCCH-H, CH₃-CH₂, H₂CCH₂-H, CH₂-X, CHX-X, CX₂-H, and CX₂-X (X = F, Cl, Br, and I) bond dissociation energies of radicals by ca. 15 kJ mol⁻¹, as expected. However, the overall RMS deviation for an even larger set including C-C, C-H, and C-X bonds of radical species was reduced to ca. 10 kJ mol⁻¹ by applying the above energy corrections, suggesting that levels of theory employing the B3P86 functional constitute a computationally effective means of prediction of bond dissociation energies even for large open-shell species, provided that suitable empirical corrections are applied. As an extension of the present work, the accuracy of bond dissociation energies calculated by the B3P86 functional for molecules containing most main-group elements is currently investigated by our group.

Conclusion

A large number of DFT functionals and several post-SCF electron correlation methods in combination with a variety of basis sets was examined in calculations of bond dissociation energies and enthalpies of formation for halogenated molecules, giving particular emphasis on the computational efficiency. A significant improvement in the accuracy of bond dissociation energy calculations for closed-shell molecules was presented by the B3P86 functional in combination with large basis sets, augmented with diffusion, and polarization functions. The B3P86/6-311++G(2df,p) and B3P86/6-311++G(3df,2p) levels of theory were found to be the most accurate, possessing systematic deviations from the experimental values which could be partly compensated by empirically increasing the total electronic energy of radicals. For the B3P86/6-311++G(2df,p) level of theory, an empirical correction of the form $N_e \cdot 9 \times 10^{-5}$ Hartrees (N_e is the total number of electrons of the radical) was found to be sufficient to lower the RMS deviation to almost 8.0 kJ mol⁻¹ for a set of 60 bond dissociation energies for 41 molecules. The level of theory chosen for the geometry optimization and vibrational frequencies calculation steps had a negligible effect on the accuracy of the calculated bond dissociation energies. Moreover, the use of the B3P86 functional was found to be superior to B3LYP and MP2 method for the geometry optimization step, with the B3P86/LanL2DZG(d) level being particularly attractive since it combines computational efficiency with accuracy of the calculated structural parameters.

The enthalpies of formation were more accurately calculated by G2 theory and levels of theory employing the B3PW91 functional (closely followed by B3LYP). However, the use of the B3P86 functional leads to enthalpies of formation underestimated by ca. 30 kJ mol⁻¹, an effect attributed to the significant overestimation of the bond dissociation energies in small radical systems.

TABLE 12: Calculated Bond Dissociation Energies (in kJ mol⁻¹) at 298.15 K and the Corresponding Deviations from Experimental Values Available, at the B3P86/6-311++G(2df,p) Level of Theory, for a Larger Set of Molecules^a

bond	experimental value ^b	B3P86/6-311++G(2df,p)		B3P86/6-311++G(2df,p) empirically corrected ^c	
		calculated	deviation	calculated	deviation
H-H	436.0 ± 0.01	444.9	8.9	444.9	8.9
F-F	158.8 ± 0.4	160.9	2.2	160.9	2.2
Cl-Cl	242.6 ± 0.01	245.3	2.7	245.3	2.7
Cl-F	251.0 ± 4.0	258.7	7.7	258.7	7.7
Br-Br	192.8 ± 0.2	194.6	1.7	194.6	1.7
Br-F	249.7 ± 4.0	247.8	-1.9	247.8	-1.9
Br-Cl	218.5 ± 4.0	221.1	2.6	221.1	2.6
I-I	151.1 ± 0.1	145.5	-5.6	145.5	-5.6
I-F	280.9 ± 4.0	257.0	-23.9	257.0	-23.9
I-Cl	210.6 ± 4.0	206.6	-4.0	206.6	-4.0
I-Br	177.7 ± 4.0	174.1	-3.6	174.1	-3.6
H-F	569.9 ± 0.8	572.0	2.1	572.0	2.1
H-Cl	431.6 ± 0.1	435.9	4.3	435.9	4.3
H-Br	366.3 ± 0.2	371.6	5.3	371.6	5.3
H-I	298.4 ± 0.1	304.5	6.1	304.5	6.1
CH ₃ -H	438.6 ± 1.1	441.7	3.2	443.9	5.3
CH ₃ CH ₂ -H	420.9 ± 2.1	422.1	1.2	426.1	5.2
CH ₃ -CH ₃	375.2 ± 2.1	371.3	-3.9	375.6	0.4
CH ₃ CH ₂ -CH ₃	369.4 ± 2.3	359.2	-10.2	365.4	-4.0
CH ₃ CH ₂ CH ₂ -H	422.7 ± 2.9	422.8	0.1	428.8	6.1
CH ₃ CHCH ₃ -H	412.7 ± 2.3	406.5	-6.2	412.4	-0.3
H ₂ C=CH-H	464.5 ± 3.7	463.1	-1.4	466.7	2.2
CH ₂ -CH ₂	720.3 ± 3.3	721.3	1.0	721.3	1.0
HC≡C-H	468.2 ± 3.3	570.3	13.0	573.4	16.0
CH-CH	961.5 ± 5.9	975.3	13.8	978.6	17.1
CH ₂ F-H	418.8 ± 9.8	422.1	3.3	426.2	7.3
CH ₃ -F	459.4 ± 5.1	465.0	5.6	467.1	7.7
CH ₂ Cl-H	423.0 ± 4.3	415.0	-8.0	420.9	-2.1
CH ₃ -Cl	350.7 ± 1.2	349.9	-0.8	352.0	1.3
CH ₂ Br-H	419.7 ± 4.3	419.9	0.3	430.1	10.4
CH ₃ -Br	291.9 ± 1.3	291.9	0.1	294.0	2.2
CH ₂ I-H	421.3 ± 6.8	407.4	-13.9	421.8	0.5
CH ₃ -I	238.2 ± 1.7	222.0	-16.1	224.2	-14.0
CHF ₂ -H	426.0 ± 4.5	421.5	-4.5	427.4	1.4
CH ₂ F-F	496.6 ± 8.6	497.9	1.3	501.9	5.3
CHCl ₂ -H	409.6 ± 5.2	398.7	-10.9	408.4	-1.2
CH ₂ Cl-Cl	338.0 ± 4.5	325.1	-13.0	331.0	-7.0
CHBr ₂ -H	417.2 ± 12.9	402.8	-14.4	421.0	3.8
CH ₂ Br-Br	290.1 ± 9.9	265.2	-24.9	275.4	-14.7
CHI ₂ -H	433.9 ± 10.1	399.5	-34.4	426.2	-7.7
CH ₂ I-I	206.3 ± 7.9	203.3	-3.1	217.7	11.4
CF ₃ -H	444.8 ± 15.6	441.2	-3.6	449.0	4.2
CHF ₂ -F	533.8 ± 5.7	525.8	-8.0	531.7	-2.1
CF ₃ -F	542.3 ± 15.6	535.9	-6.4	543.7	1.4
CCl ₃ -H	400.7 ± 4.7	385.3	-15.4	398.7	-1.9
CHCl ₂ -Cl	320.7 ± 6.4	301.5	-19.2	311.2	-9.5
CCl ₃ -Cl	296.8 ± 4.7	268.9	-27.9	282.3	-14.4
CBr ₃ -H	393.7 ± 12.7	384.2	-9.5	410.4	16.7
CHBr ₂ -Br	275.0 ± 12.9	236.2	-38.9	254.4	-20.7
CBr ₃ -Br	228.8 ± 9.6	199.9	-28.9	226.2	-2.6
Cl ₃ -H	-	374.2	-	413.2	-
CHI ₂ -I	-	166.4	-	193.1	-
Cl ₃ -I	-	117.4	-	156.4	-
CF ₃ -CH ₃	424.1 ± 15.5	415.8	-8.3	425.8	1.7
CF ₃ CH ₂ -H	447.9 ± 5.9	443.4	-4.5	453.1	5.2
CF ₃ -CF ₃	403.3 ± 21.9	381.4	-21.9	397.0	-6.3
CF ₃ CF ₂ -F	532.1 ± 6.4	514.4	-17.7	527.9	-4.2
CF ₃ -Cl	358.9 ± 15.7	355.1	-3.8	362.9	4.0
CF ₃ -Br	290.5 ± 15.4	286.5	-4.1	294.3	3.7
CF ₃ -I	225.6 ± 15.4	215.9	-9.7	223.7	-1.9
		Total Deviation			
RMS		-	12.7	-	8.0
MAD		-	9.1	-	5.9
AVD		-	-6.1	-	0.6
MND		-	-38.9	-	-23.9
MPD		-	13.8	-	17.1

^a Molecular structures optimized and vibrational frequencies calculated at the B3P86/LanL2DZG(d) level. ^b Obtained from the corresponding enthalpies of formation from ref 11, except for the following: monohalomethyl radicals, CHF₂, CHCl₂, CHBr₂, CBr₃, CH₂Br₂, CF₃CH₂, CF₃CF₂, and CF₃CH₃ (ref 6); CH₃Br (ref 21), and CH₃I (ref 22); alkyl and vinyl radicals (ref 84); alkanes (ref 85); CH₂I₂ and Cl₄ (ref 86); CHBr₃ (ref 87); and CBr₄ (ref 88). ^c Increasing the total electronic energies of the radicals by $N_e \cdot 9 \times 10^{-5}$ Hartrees (where N_e is the total number of electrons of the radical).

The relative ordering of all 42 DFT functionals in respect to their accuracy in thermochemical calculations suggests that the B3P86 functional clearly surpasses all other functionals for the calculation of bond dissociation energies for closed-shell molecules, while B3PW91 appears marginally better than its closest competitors in the calculation of enthalpies of formation for stable molecules and radicals.

References and Notes

- Molina, M. J.; Molina, L. T.; Kolb, C. E. *Annu. Rev. Phys. Chem.* **1996**, *47*, 327–367.
- Kley, D. *Science* **1997**, *276*, 1043–1045.
- Spicer, C. W.; Chapman, E. G.; Finlayson-Pitts, B. J.; Plastryde, R. A.; Hubbe, J. M.; Fast, J. D.; Berkowitz, C. M. *Nature* **1998**, *394*, 353–356.
- Rowland, F. S. *Annu. Rev. Phys. Chem.* **1991**, *42*, 731–768.
- Barrie, L. A.; Bottenheim, J. W.; Schnell, R. C.; Crutzen, P. J.; Rasmussen, R. A. *Nature*, **1988**, *334*, 138–141.
- DeMore, W. B.; Sander, S. P.; Golden, D. M.; Hampson, R. F.; Kurylo, M. J.; Howard, C. J.; Ravishankara, A. R.; Kolb, C. E.; Molina, M. J. *Chemical Kinetics and Photochemical Data for Use in Stratospheric Modelling*; JPL Publication 97–4; 1997.
- Tschuikow-Roux, E.; Yano, T.; Niedzelski, J. *J. Phys. Chem.* **1984**, *88*, 1408–1414.
- Atkinson, R. *Chem. Rev.* **1985**, *85*, 69–201.
- Senkan, S. M.; Quam, D. J. *Phys. Chem.* **1992**, *96*, 10837–10842.
- Chase, M. W., Jr. *J. Phys. Chem. Ref. Data* **1998**, *9*, 1–1951.
- NIST Standard Reference Database Number 69 - February 2000 Release* (<http://webbook.nist.gov/chemistry/>).
- McGrath, M. P.; Radom, L. *J. Chem. Phys.* **1991**, *94*, 511–516.
- Berry, R. J.; Burgess, D. R. F., Jr.; Nyden, M. R.; Zachariah, M. R.; Schwartz, M. J. *Phys. Chem. A* **1995**, *99*, 17145–17150.
- Dixon, D. A.; Feller, D.; Sandrone, G. *J. Phys. Chem. A* **1999**, *103*, 4744–4751.
- Curtiss, L. A.; McGrath, M. P.; Blaudeau, J.-P.; Davis, N. E.; Binning, Jr. R. C.; Radom, L. *J. Chem. Phys.* **1995**, *103*, 6104–6113.
- Glukhovtsev, M. N.; Pross, A.; McGrath, M. P.; Radom, L. *J. Chem. Phys.* **1995**, *103*, 1878–1885.
- Curtiss, L. A.; Raghavachari, K.; Redfern, P. C.; Pople, J. A. *J. Chem. Phys.* **1997**, *106*, 1063–1079.
- Redfern, P. C.; Blaudeau, J.-P.; Curtiss, L. A. *J. Phys. Chem. A* **1997**, *101*, 8701–8705.
- Petersson, G. A.; Malick, D. K.; Wilson, W. G.; Ochterski, J. W.; Montgomery, J. A., Jr.; Frisch, M. J. *J. Chem. Phys.* **1998**, *109*, 10570–10579.
- McGivern, W. S.; Derecskei-Kovacs, A.; North, S. W.; Francisco, J. S. *J. Phys. Chem. A* **2000**, *104*, 436–442.
- Ferguson, K. C.; Okafu, E. N.; Whittle, E. *J. Chem. Soc., Faraday Trans. 1* **1973**, *69*, 295–301.
- Cox, J. D.; Pilcher, G. *Thermochemistry of Organic and Organometallic Compounds*; Academic Press: New York, 1970.
- Hohenberg, P.; Sham, L. *J. Phys. Rev. B* **1964**, *136*, 864.
- Kohn, W.; Sham, L. *J. Phys. Rev. A* **1965**, *140*, 1133.
- Perdew, J. P.; Wang, Y. *Phys. Rev. B* **1992**, *45*, 13244.
- Becke, A. D. *J. Chem. Phys.* **1992**, *96*, 2155.
- Becke, A. D. *J. Chem. Phys.* **1992**, *97*, 9173.
- Möller, C.; Plesset, M. S. *Phys. Rev.* **1934**, *46*, 618.
- Frisch, M. J.; Head-Gordon, M.; Pople, J. A. *Chem. Phys. Lett.* **1990**, *166*, 281.
- Krishnan, R.; Pople, J. A. *Int. J. Quantum Chem.* **1978**, *14*, 91.
- Pople, J. A.; Head-Gordon, M.; Raghavachari, K. *J. Chem. Phys.* **1987**, *87*, 5968.
- Pople, J. A.; Krishnan, R.; Schlegel, H. B.; Binkley, J. S. *Int. J. Quantum Chem.* **1978**, *XIV*, 545.
- Bartlett, R. J.; Purvis, G. D. *Int. J. Quantum Chem.* **1978**, *14*, 516.
- Binkley, J. S.; Pople, J. A.; Hehre, W. J. *J. Am. Chem. Soc.* **1980**, *102*, 939.
- Dobbs, K. D.; Hehre, W. J. *J. Comput. Chem.* **1987**, *8*, 880.
- Schaefer, A.; Huber, C.; Ahlrichs, R. *J. Chem. Phys.* **1994**, *100*, 5829.
- McLean, A. D.; Chandler, G. S. *J. Chem. Phys.* **1980**, *72*, 5639.
- Krishnan, R.; Binkley, J. S.; Seeger, R.; Pople, J. A. *J. Chem. Phys.* **1980**, *72*, 650.
- Woon, D. E.; Dunning, Jr. T. H. *J. Chem. Phys.* **1993**, *98*, 1358.
- Peterson, K. A.; Woon, D. E.; Dunning, T. H., Jr. *J. Chem. Phys.* **1994**, *100*, 7410.
- Wilson, A.; van Mourik, T.; Dunning, T. H., Jr. *J. Mol. Struct. (THEOCHEM)* **1997**, *388*, 339.
- Wilson, A. K.; Woon, D. E.; Peterson, K. A.; Dunning, Jr. T. H. *J. Chem. Phys.*, **1999**, *110*, 7667.
- Dunning, T. H., Jr.; Hay, P. J. In *Modern Theoretical Chemistry*; Schaefer, H. F., III, Plenum: N. Y. 1976.
- Hay, P. J.; Wadt, W. R. *J. Chem. Phys.* **1985**, *82*, 270.
- Leininger, T.; Nicklass, A.; Stoll, H.; Dolg, M.; Schwerdtfeger, P. *J. Chem. Phys.* **1996**, *105*, 1052.
- Cundari, T. R.; Stevens, W. J. *J. Chem. Phys.* **1993**, *98*, 5555.
- Frisch, M. J.; Trucks, G. W.; Schlegel, H. B.; Gill, P. M. W.; Johnson, B. G.; Robb, M. A.; Cheeseman, J. R.; Keith, T.; Petersson, G. A.; Montgomery, J. A.; Raghavachari, K.; Al-Laham, M. A.; Zakrzewski, V. G.; Ortiz, J. V.; Foresman, J. B.; Cioslowski, J.; Stefanov, B. B.; Nanayakkara, A.; Challacombe, M.; Peng, C. Y.; Ayala, P. Y.; Chen, W.; Wong, M. W.; Andres, J. L.; Replogle, E. S.; Gomperts, R.; Martin, R. L.; Fox, D. J.; Binkley, J. S.; Defrees, D. J.; Baker, J.; Stewart, J. P.; Head-Gordon, M.; Gonzalez, C.; Pople, J. A. *Gaussian 94*, Revision D.4; Gaussian, Inc.: Pittsburgh, PA, 1995.
- Frisch, M. J.; Trucks, G. W.; Schlegel, H. B.; Scuseria, G. E.; Robb, M. A.; Cheeseman, J. R.; Zakrzewski, V. G.; Montgomery, J. A., Jr.; Stratmann, R. E.; Burant, J. C.; Dapprich, S.; Millam, J. M.; Daniels, A. D.; Kudin, K. N.; Strain, M. C.; Farkas, O.; Tomasi, J.; Barone, V.; Cossi, M.; Cammi, R.; Mennucci, B.; Pomelli, C.; Adamo, C.; Clifford, S.; Ochterski, J.; Petersson, G. A.; Ayala, P. Y.; Cui, Q.; Morokuma, K.; Malick, D. K.; Rabuck, A. D.; Raghavachari, K.; Foresman, J. B.; Cioslowski, J.; Ortiz, J. V.; Baboul, A. G.; Stefanov, B. B.; Liu, G.; Liashenko, A.; Piskorz, P.; Komaromi, I.; Gomperts, R.; Martin, R. L.; Fox, D. J.; Keith, T.; Al-Laham, M. A.; Peng, C. Y.; Nanayakkara, A.; Gonzalez, C.; Challacombe, M.; Gill, P. M. W.; Johnson, B.; Chen, W.; Wong, M. W.; Andres, J. L.; Gonzalez, C.; Head-Gordon, M.; Replogle, E. S.; Pople, J. A. *Gaussian 98*, Revision A.7; Gaussian, Inc.: Pittsburgh, PA, 1998.
- Environmental Molecular Sciences Laboratory* (<http://www.emsl.pnl.gov/>), March 2000.
- Visscher, L.; Dyall, K. G. *J. Chem. Phys.* **1996**, *104*, 9040–9046.
- Visscher, L.; Styszyński, J.; Nieuwpoort, W. C. *J. Chem. Phys.* **1996**, *105*, 1987–1994.
- Visscher, L. Personal communication, July 2000.
- Boys, S. F.; Bernardi, F. *Mol. Phys.* **1970**, *19*, 553–566.
- Moore, C. E. *Atomic Energy Levels*; NSRDS-NBS 35; National Bureau of Standards: Washington, DC, 1971; Vols. II and III.
- Curtiss, L. A.; Raghavachari, K.; Trucks, G. W.; Pople, J. A. *J. Chem. Phys.* **1991**, *94*, 7221–7230.
- Curtiss, L. A.; Carpenter, J. E.; Raghavachari, K.; Pople, J. A. *J. Chem. Phys.* **1992**, *96*, 9030.
- Foresman, J. B.; Frisch, M. J. *Exploring Chemistry with Electronic Structure Methods*, 2nd ed.; Gaussian, Inc.: Pittsburgh, PA, 1996.
- CRC Handbook of Chemistry and Physics*; CRC Press: Boca Raton, FL, 1995.
- Li, Z.; Francisco, J. S. *J. Chem. Phys.* **1999**, *110*, 817–822.
- Perdew, J. P. *Phys. Rev. B* **1986**, *33*, 8822–8824.
- Becke, A. D. *J. Chem. Phys.* **1993**, *98*, 5648–5652.
- Becke, A. D. *Phys. Rev. A* **1988**, *38*, 3098.
- Lee, C.; Yang, W.; Parr, R. G. *Phys. Rev. B* **1988**, *37*, 785.
- Miehlich, B.; Savin, A.; Stoll, H.; Preuss, H. *Chem. Phys. Lett.* **1989**, *200*, 157.
- Perdew, J. P.; Chevary, J. A.; Vosko, S. H.; Jackson, K. A.; Pederson, M. R.; Singh, D. J.; Fiolhais, C. *Phys. Rev. B* **1992**, *B 46*, 6671.
- Perdew, J. P.; Burke, K.; Wang, Y. *Phys. Rev. B* **1996**, *54*, 16533.
- Hehre, W. J.; Radom, L.; Schleyer, P. v. R.; Pople, J. A. *Ab-initio Molecular Orbital Theory*; Wiley-Interscience: New York, 1986.
- Davidson, E. R.; Feller, D. *Chem. Rev.* **1986**, *86*, 681–696.
- Schwenke, D. W.; Truhlar, D. G. *J. Chem. Phys.* **1985**, *82*, 2418–2426.
- Frisch, M. J.; Del Bene, J. E.; Binkley, J. S.; Schaefer, H. F., III. *J. Chem. Phys.* **1986**, *84*, 2279–2289.
- Slater, J. C. *Quantum Theory of Molecules and Solids, Vol 4: The Self-Consistent Field for Molecules and Solids*; McGraw-Hill: New York, 1974.
- Lazarou, Y. G.; Papadimitriou, V. C.; Pross, A. V.; Papagian-nakopoulos, P. Manuscript in preparation.
- DiLabio, G. A.; Pratt, D. A. *J. Phys. Chem. A* **2000**, *104*, 1938–1943.
- Altmann, J. A.; Handy, N. C.; Ingamells, V. E. *Mol. Phys.* **1997**, *92*, 339–352.
- Andzelm, J.; Klobukowski, M.; Radzio-Andzelm, E. *J. Comput. Chem.* **1984**, *5*, 146.
- Bauchschlicher, C. W., Jr.; Partridge, H. *J. Chem. Phys.* **1995**, *103*, 1788–1791.
- Rabuck, A. D.; Scuseria, G. E. *Chem. Phys. Lett.* **1999**, *309*, 450–456.
- Nyden, M. R.; Petersson, G. A. *J. Chem. Phys.* **1981**, *75*, 1843.
- Ochterski, J. W.; Petersson, G. A.; Montgomery, J. A., Jr. *J. Chem. Phys.* **1996**, *104*, 2598.
- Fast, P. L.; Sanchez, M. L.; Truhlar, D. G. *J. Chem. Phys.* **1999**, *111*, 2921–2925.

(81) Huber, K. P.; Herzberg, G. *Molecular Spectra and Molecular Structure, IV. Constants of Diatomic Molecules*; Van Nostrand Reinhold Co.: New York, 1979.

(82) Murray, K. K.; Leopold, D. G.; Miller, T. M.; Lineberger, W. C. *J. Chem. Phys.* **1988**, *89*, 5442.

(83) Gilles, M. K.; Ervin, K. M.; Ho, J.; Lineberger, W. C. *J. Phys. Chem.* **1992**, *96*, 1130.

(84) Tsang, W. In *Energetics of Organic Free Radicals*; Martinho Simoes, J. A., Greenberg, A., Liebman, J. F., Eds.; Blackie Academic and

Professional: London, 1996; pp 22–58.

(85) Pittam, D. A.; Pilcher, G. *J. Chem. Soc., Faraday Trans. 1* **1972**, *68*, 2224–2229.

(86) Kudchadker, S. A.; Kudchadker, A. P. *J. Phys. Chem. Ref. Data* **1976**, *5*, 529–530.

(87) Papina, T. S.; Kolesov, V. P.; Golovanova, Yu. G. *Russ. J. Phys. Chem. (Engl. Transl.)* **1982**, *56*, 1666–1668.

(88) Bickerton, J.; Minas Da Piedade, M. E.; Pilcher, G. *J. Chem. Thermodyn.* **1984**, *16*, 661–668.